Arab J. Nucl. Sci. Appl., Vol. 58, 4, 17-28 (2025)

ISSN 1110-0451

Arab Journal of Nuclear Sciences and Applications

Web site: ajnsa.journals.ekb.eg

(E S N S A)

Estimation of Safety Parameters of IRIS Reactor Core with Reduced Fuel Length

Ahmed M. Refaey, Hend M. Saad, Samaa A. Wasfy, Afaf A.E. Ateya and Salwa H. Abdel-Latif.

Nuclear & Radiological Safety Research Center, Egyptian Atomic Energy Authority (EAEA), Cairo, Egypt

ARTICLE INFO

Article history:

Received: 9th July 2025

Accepted: 17th Aug. 2025

Available online: 1st Sept. 2025

Keywords:

IRIS core,

neutronic and thermal hydraulic calculations,

MCNP6 code,

ANSYS code,

axial power,

temperature and stress distribution.

ABSTRACT

In this work, neutronics and thermal-hydraulic behaviors are analyzed to illustrate the effect of reduced- fuel rod length for the International Reactor Innovative Secure (IRIS) core. The IRIS core design considered is 1000 MWt and fueled with up to 4.95% enriched uranium dioxide. A three-dimensional Monte Carlo computer code, (MCNP6), is coupled with the thermal-hydraulics code (ANSYS FLUENT), to calculate the safety parameters namely: the effective multiplication factor, axial power distribution, power peaking factor, (fuel, clad, and coolant) temperatures. The results are used to calculate the mechanical parameters such as stresses and fuel rod deformation due to the thermal stress. Stress and deformation are established with the ANSYS-STATIC structure module. In the present work, five cases are considered for the reference reactor core configurations with different fuel rod lengths. In each case, a set value for the ratio of fuel rod length (H) to core diameter (D) by varying the fuel rod length from 4.2672 m to 2 m is used. This is done in five stages depending on the length of the fuel rod: H/D = 1.72, 1.5, 1.25, 1.00, and 0.8, respectively. The results obtained with detailed modeling of the IRIS reactor core are very promising and will increase the accuracy in predicting the main safety parameters with the coupled system codes MCNP6/ANSYS. The results showed that the ratio H/D of the fuel rod must not be less than 1.25.

1- INTRODUCTION

Over the past 20 years, research institutes worldwide have produced a huge number of small and medium-sized reactors (SMRs) that offer flexible, cost-effective energy for a variety of applications. The majority of light-water cooled SMRs use the mature rod-type fuel assembly used in large PWRs. Each SMR has a different fuel assembly height. Standard 17X17 PWR fuel assemblies with active core heights of 4.27 or 3.66 meters are used in some SMR designs, whereas Reduced-Height PWR fuel assemblies with active core heights of 2.4, 1.9, 1.4, etc. are used by others.

Analysis of the neutronics and thermal-hydraulic behavior of the SMRs is required for the design's economics and safety. Coolant enthalpy, density, mass, velocity, liquid temperature, vapor void percentage, static pressure distribution, and DNBR distributions can all be predicted using subchannel analysis. [1] Whereas, the effective multiplication factor (k_{eff}), the reactivity coefficients, the neutron flux, the radial and axial power distribution can be predicted using Monte Carlo technique.

Due to the impact of temperature on neutronic parameters, neutronic calculations must be performed in conjunction with thermal-hydraulic calculations. Most neutronic simulation codes are capable of modeling 3D reactor core configurations while considering all geometric and material composition specifications. However, since nuclear reaction cross-sections depend on temperature, these codes cannot compute radial or axial temperature variations on their own, making accurate modeling of temperature distribution essential for precise simulation.

On the other hand, thermal-hydraulic codes can calculate temperature variations in different reactor components (fuel, cladding, and coolant), but they require the power distribution as an input, which is obtained from neutronic codes. Therefore, coupling both

Corresponding author: samaaahmedwasfy1812@yahoo.com
DOI: 10.21608/ajnsa.2025.402240.1891

types of codes allows for accurate modeling of feedback effects without needing to modify the codes themselves. This coupling between neutron transport and thermal-hydraulic codes is widely used across various reactor types. Additionally, several coupled Monte Carlo neutronics/thermal-hydraulics systems have been developed to address a range of complex problems. [2-6]

In the present work, neutronics and thermal hydraulic models are created to simulate different five cases for IRIS reactor. Each case has the same material composition but different fuel rod lengths. The coupled codes are applied to IRIS reactor core for steady state calculations. The k_{eff} and axial power distribution are determined in each case using MCNP6 , and then it is provided to ANSYS to calculate the variation of the actual temperature values for (fuel, clad and coolant). The increase in temperature led to thermal stress, the stress distribution and deformation are established with the ANSYS-STATIC structure module.

2- DESCRIPTION OF THE IRIS REACTOR

The International Reactor Innovative and Secure (IRIS) is a modular, integral light water reactor designed to meet the four major objectives set by the U.S. Department of Energy for Generation IV nuclear systems: proliferation resistance, enhanced safety, economic competitiveness, and reduced waste. IRIS is being developed by an international consortium that includes industry, laboratory, university, and utility organizations, with Westinghouse leading the project [7].

IRIS is designed to have a 1000 MW thermal power output. The reactor core contains 89 fuel assemblies (FAs), each arranged in a 15x15 square matrix. Out of the 225-unit cells, 204 are fuel cells, the central position is occupied by an instrumentation tube (IT), and the remaining 20 positions are occupied by guide thimbles (GT). The active fuel height is 426.72 cm, with an axially uniform enrichment of 4.95 w/o U-235. The total core height, including the top and bottom axial reflector regions, is 506.72 cm.

The radial reflector is modeled using cells that match the dimensions of fuel assemblies. It consists of a homogeneous mixture of 50% water and 50% stainless steel by volume, serving to reflect neutrons back into the core and improve neutron economy. The fuel pin model includes uranium dioxide fuel pellets enclosed in zirconium cladding, with water serving as a moderator between pins. The assembly also includes guide thimbles (GTs) for control rods and instrumentation tubes (ITs), which are modeled accordingly.

The core barrel is made of SS-304 steel, with a thickness of 5 cm. It has an inner radius of 137.5 cm and an outer radius of 142.5 cm. The RPV cladding (Reactor Pressure Vessel) is also made of SS-304, with a thickness of 0.6 cm; its inner and outer radii are 310.5 cm and 311.1 cm, respectively. The RPV itself is constructed from low-carbon steel, with a thickness of 28.5 cm; the inner and outer radii of the RPV are 311.1 cm and 339.6 cm, respectively. The down comer is 16.8 cm thick. A brief description of the major components of the IRIS plant is summarized in Table 1 and Table 2.[8-9].

Table (1): IRIS Basic Components

DESIGN PARAMETERS	Value
Reactor Thermal Power, MWt	1000
Reactor Electric Power, MWe	335
Reactor Coolant Flow, kg/s	4481
Reactor Coolant Pressure MPa	15.5
Core Outlet Temperature, ^oC	330
Vessel Outlet Temperature, ^oC	327.9
Core Average Temperature, ^oC	311
Vessel Average Temperature, ^oC	309.9
Vessel/Core Inlet Temperature, ^oC	292
Steam Generator Outlet Temperature, ^oC	292
Steam Generator Model	Modular Helical Coil
S.G number of modules	8

Table (2): Summary of IRIS Geometry

Outer radius of fuel	0.46482 cm
Outer radius of gap	0.47371 cm
Outer radius of clad	0.53721 cm
Fuel rod pitch	1.50419 cm
Inner radius of Guide thimble (GT), instrumentation tube (IT)	0.68072 cm
Outer radius of Guide thimble (GT), instrumentation tube (IT)	0.72390 cm
fuel assembly pitch	22.664 cm

3- COMPUTATIONAL TOOLS

This section will present a brief overview of Monte Carlo code MCNP6 and thermal-hydraulics and mechanical code ANSYS.

3.1- MCNP6 Code

MCNP6 offers exact geometry modeling, the use of continuous energy cross sections, and the ability to track and tally neutrons on an unstructured mesh. It can be applied for all core calculations using established cross-section libraries. [10] All core calculations refers to the set of computational analyses performed to model, simulate, and evaluate the behavior and performance of a nuclear reactor core during operation. These calculations are essential for design, safety analysis, and operation of the reactor.

MCNP6 can be used to calculate the neutron multiplication factor, fuel burnup, and flux and power distributions within the reactor. Additionally, it incorporates features that support thermal-hydraulic feedback, making it a powerful tool for nuclear and thermal analysis in reactor simulations.

3.2- Thermal-hydraulics ANSYS code

ANSYS, developed by the U.S. Nuclear Regulatory Commission (NRC), includes the ANSYS FLUENT software, which is based on a "Finite Volume" (FV) approach. In this method, the solution domain, which refers to the fluid domain, is divided into a finite number of small "Control Volumes" (CVs) through meshing, as illustrated in Figure 4. The solution variables and fluid properties are stored at computational nodes, which are placed at the center of the CVs or arranged so that the CV faces lie midway between nodes [11].

In this study, a numerical approach using a CFD model is employed, incorporating the governing equations for the conservation of mass, momentum, and species. Due to the high flow rates, turbulent flow is assumed for all simulations, necessitating the use of Reynolds-Averaged Navier–Stokes (RANS) equations, used to describe the behavior of turbulent fluid flow. They are widely used in engineering simulations, including nuclear reactor thermal-hydraulics, aerospace, automotive, and more. These equations are discretized using the finite volume method. The turbulence model used for the enclosed domain is the standard κ–ε model, along with standard wall functions.

4- Coupling Model Description

In the current study, two models are developed: a neutronic model and a thermal-hydraulic model, both designed to represent the IRIS reactor core. The neutronic model is employed to calculate the effective multiplication factor (keff) and the axial power distribution, while the thermal-hydraulic model is used to determine the temperature distribution across the fuel, cladding, and coolant. These two codes are coupled externally to facilitate data exchange between them.

The coupled models are created to simulate five cases. Each case contains fuel rods that have the same material composition but differ in length from each case to another. The first case has a rod length H = 426.72 cm with a ratio (H/D) = 1.72, where H is the rod length and D is the core diameter. The second case has a ratio of 1.5 where the rod length is 376.7, and for the other cases, the ratios are 1.25, 1.0, and 0.8 where the fuel rod length is 311.5, 249.08, and 200 cm, respectively. Each rod in the core is divided into 13 axial layers. The different lengths of fuel rod used are shown in figure (1).

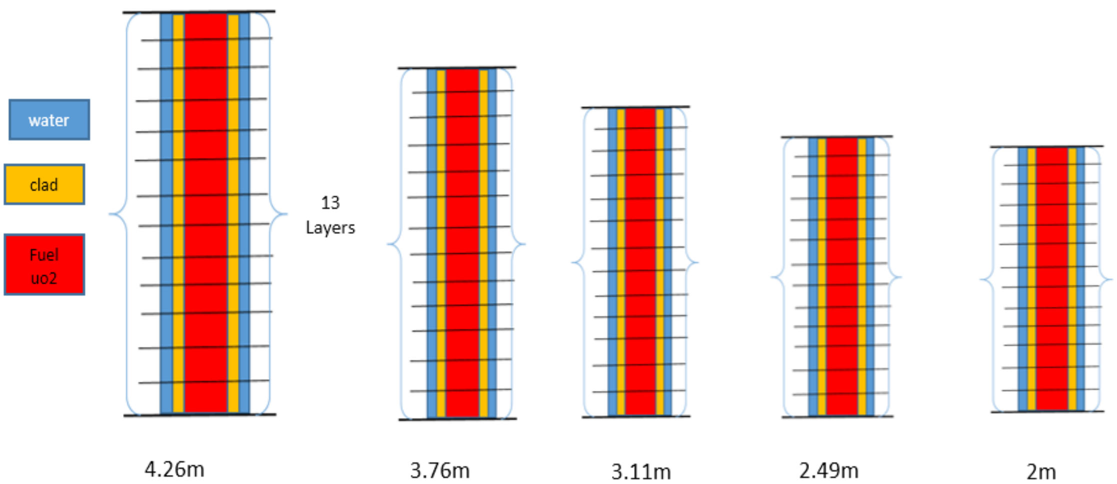

Fig. (1): Axial view for five IRIS's core fuel rod (m)

4.1. Neutronic Model

IRIS's reactor core is simulated by MCNP6 code using ENDF/B-VII.1 cross section library for the actual reactor including core barrel and RPV. MCNP6 is applied to perform criticality calculations for the reactor core by calculating the effective multiplication factor (K_{eff}) and the axial power distribution. The calculations are carried out at 600 active cycles, 100 skipped cycles and 100000 neutron per cycle [12].

Figure 2 shows a horizontal view of the simulated MCNP6 assembly model. Also, figure (3) shows horizontal and vertical views of the simulated MCNP6 model of IRIS core.

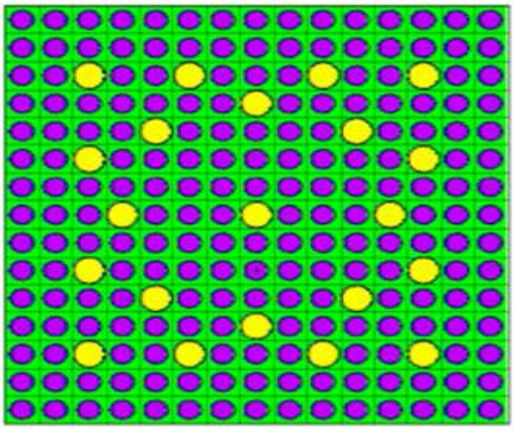

Fig. (2): Horizontal view for IRIS fuel assembly by MCNP6

4.2- Thermal-Hydraulic Model

The thermal-hydraulic parameters are investigated in forced convection for the IRIS fuel assembly within the core using the ANSYS-FLUENT 17.2 code. To address water flow issues, including temperature and density distributions, different mesh configurations and turbulence models are employed. The mesh representation of the IRIS fuel rod in ANSYS-FLUENT is shown in Figure 4.

4.3- Coupling of FLUENT Models and MCNP6

The Iterative Coupling Scheme between the MCNP6 and FLUENT codes is implemented through a series of iterations, starting with the thermal-hydraulic model in ANSYS-FLUENT followed by the neutronics model.

For first iteration, the energy profile for each of the five fuel rod length models is assumed to be constant across all axial layers, with the power of all the fuel rods being the same. The coolant temperature and pressure at the entrance are maintained constant. For each axial zone, the results provide the actual temperature distributions for the fuel, cladding, and coolant. Additionally, the coolant density is calculated based on the temperatures obtained.

These temperature and density results are then fed into the MCNP6 code to compute the axial power distributions for the five cases with varying fuel rod lengths. The power distributions are then provided as input to the FLUENT model. The next iteration begins after this step. The iterative process continues until the convergence criteria are met, allowing for the feedback of cross-section data based on the local thermal conditions.

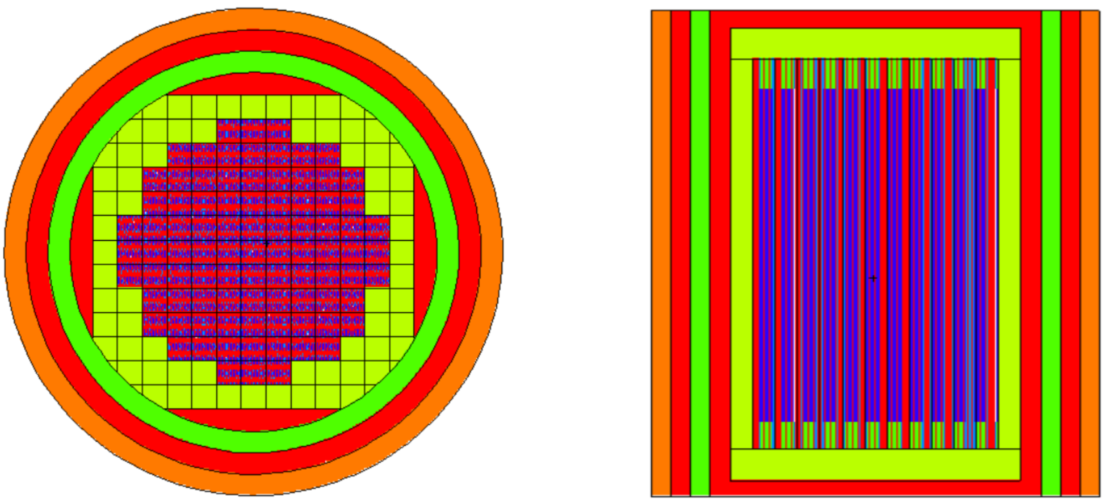

Fig. (3): IRIS Core configuration horizontal and vertical views

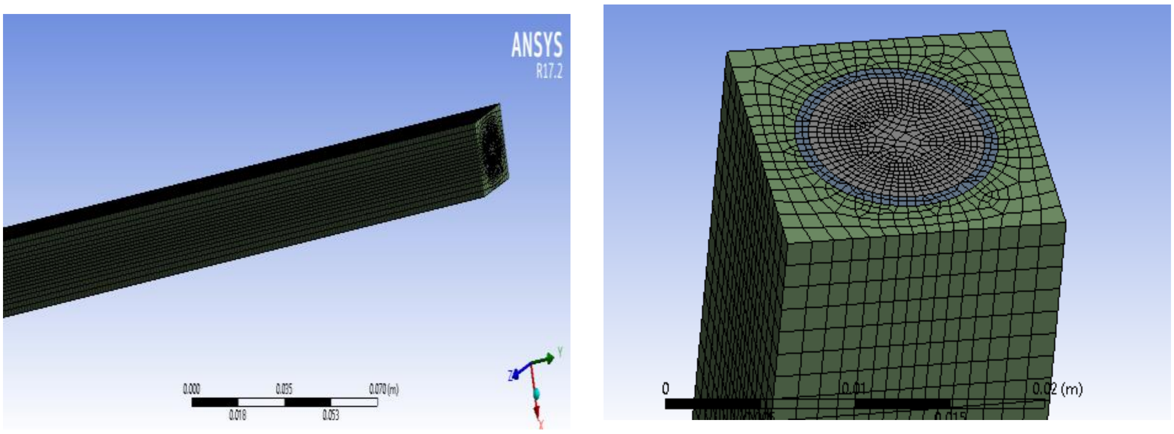

Fig. (4): representation of fuel rod with ANSYS-FLUENT mesh

$$dk_i = \frac{|k_i - k_{i-1}|}{k_i} * 100\% < 0.1\% \quad (1)$$

$$dP_i = \frac{|P_i - P_{i-1}|}{P_i} * 100\% < 1.0\% \quad (2)$$

$$dTf_i = \frac{|Tf_i - Tf_{i-1}|}{Tf_i} * 100\% < 0.5\% \quad (3)$$

Where for iteration i, k_i is the effective multiplication factor, P_i is the power [MWt], Tf_i is the fuel temperature [K]. Equations (2) and (3) are evaluated for fuel assemblies, and are applied to the whole core.[13]

5 RESULTS AND DISCUSSION

MCNP6/ANSYS-FLUENT codes are applied to IRIS reactor core for steady state calculations of five cases with different fuel rod lengths. Each case is chosen to be different in H/D ratio.

Initially, the calculation conditions are modified to verify the accuracy of the coupling method. An iterative process is employed, continuing until the convergence criteria specified in Eqs. (1)–(3) are met. The results encompass the calculations of keff, the axial power distribution, and the temperatures of the coolant, cladding, and fuel within the IRIS core.

5.1 Adjustment of the coupling conditions

5.1.1 Effective multiplication factor

The IRIS reactor core k_{eff} is obtained by MCNP6 at sufficient active neutron cycles and neutron histories as mentioned before. Figure 5 presents the variation of k_{eff} for the IRIS reactor core with the five iterations. It is clear that there are different variations for k_{eff} of the IRIS core for the first three iterations for H/D= 1.25,1, and 0.8, and the convergence is satisfied for H/D= 1.52, and 1.72, then this variation decreases till it is converged at iteration 5 where Eq. (1) is fulfilled.

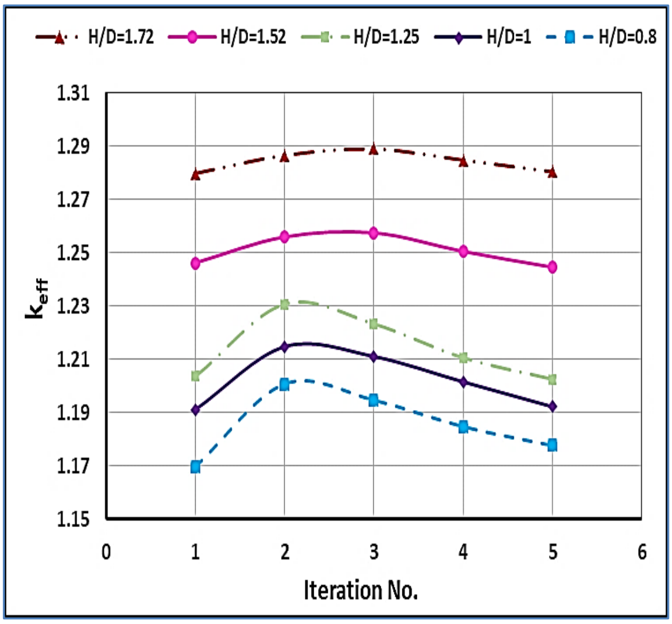

Fig. (5): Variation of k_{eff} of IRIS reactor core with iteration number

5.1.2 Axial power and temperature distribution

The coupled MCNP6/ANSYS FLUENT is tested for convergence in power and fuel temperature. Following 5 iterations along 13 axial layers in different fuel rod lengths are studied at full power conditions. From the three equations mentioned above, Di1 represents the error between iterations 2 and 1 while Di5 is the error between iterations 5 and 4.

It is found that the oscillation in thermal parameters in the first iterations is strong and gradually decreases with iteration till it reaches iteration number 5, as shown in figures (6-10).

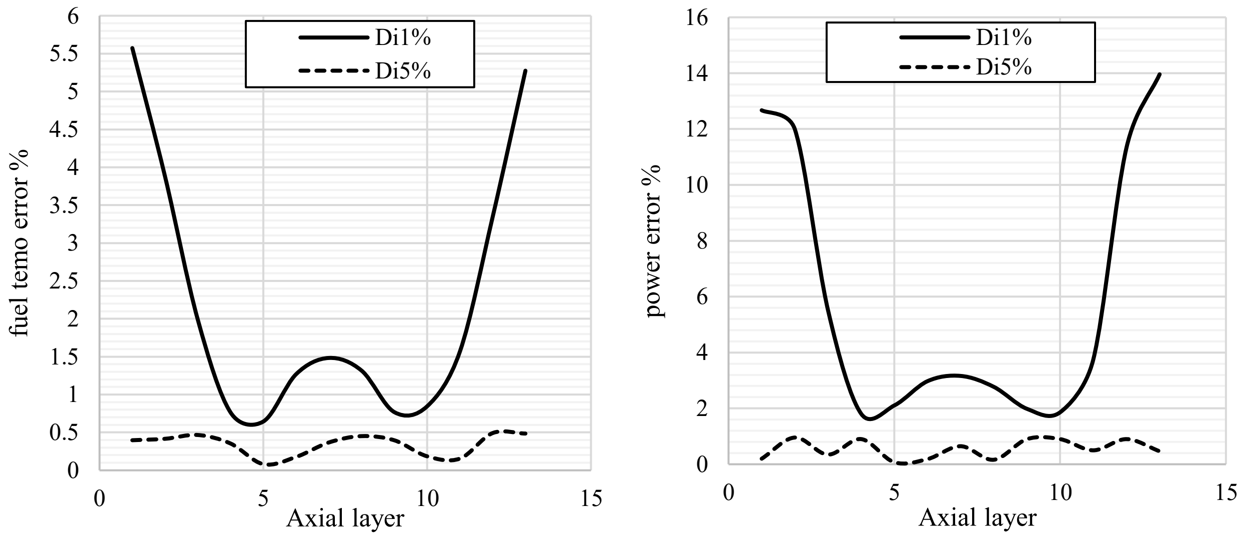

Fig. (6): Error of axial power and fuel temperature distribution, H/D=1.72

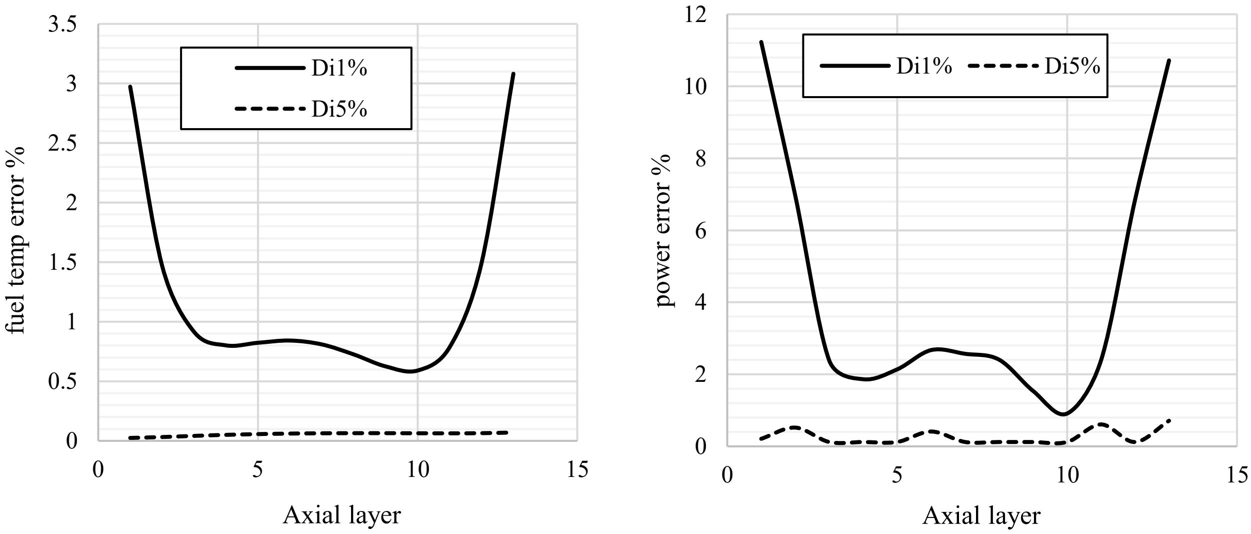

Fig. (7): Error of axial power and fuel temperature distribution, H/D= 1.5124

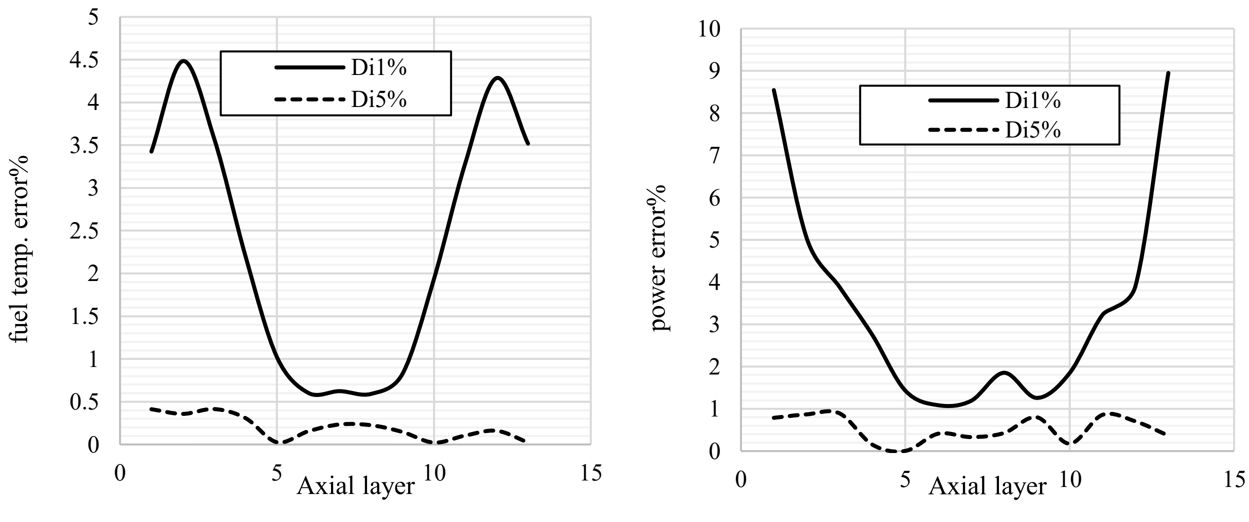

Fig. (8): Error of axial power and fuel temperature distribution/D=1.25

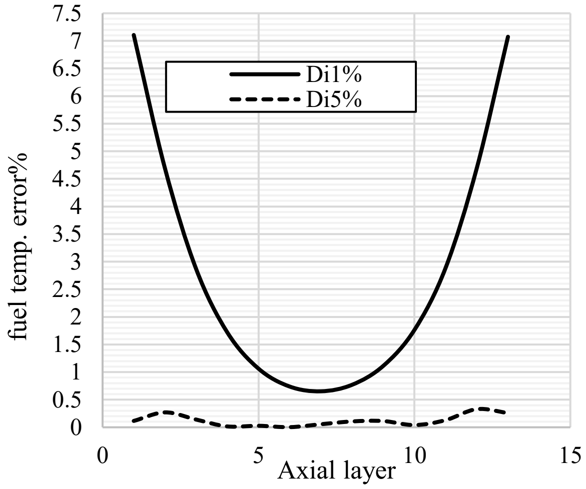

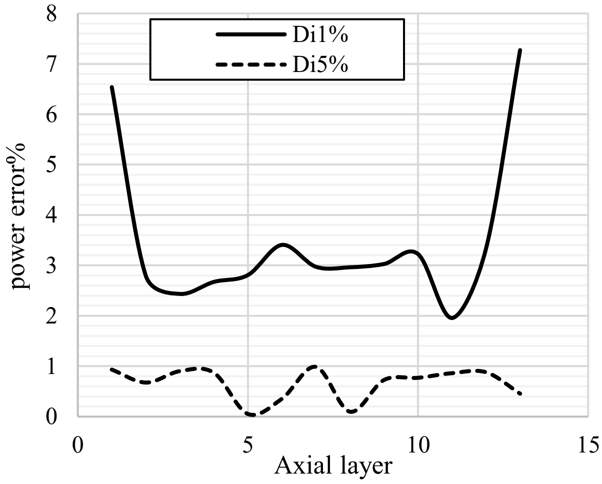

Fig. (9): Error of axial power and fuel temperature distribution, H/D=1.0

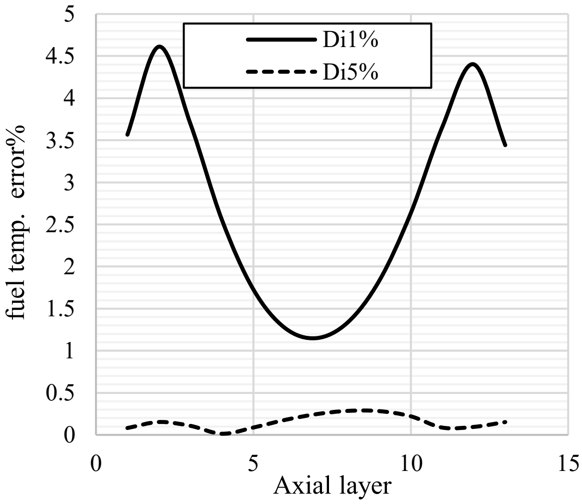

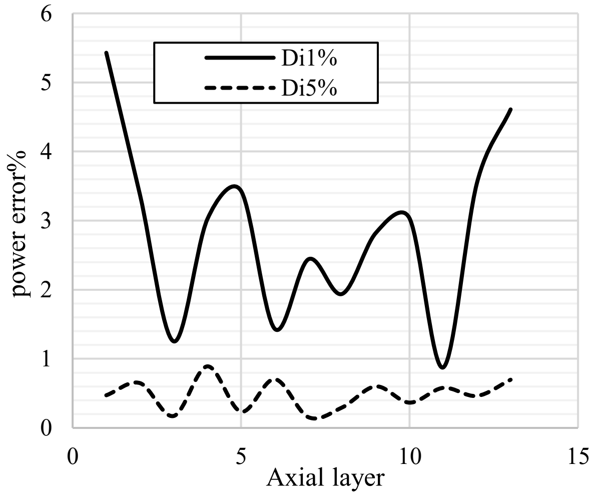

Fig. (10): Error of axial power and fuel temperature distribution, H/D=0.8

Taking into account the changes of the fuel and cladding temperatures, convergence in power occurred. So, the convergence criteria are fulfilled after iteration 5.

5.2 The effect of H/D ratios variation of fuel rods on safety parameters of IRIS

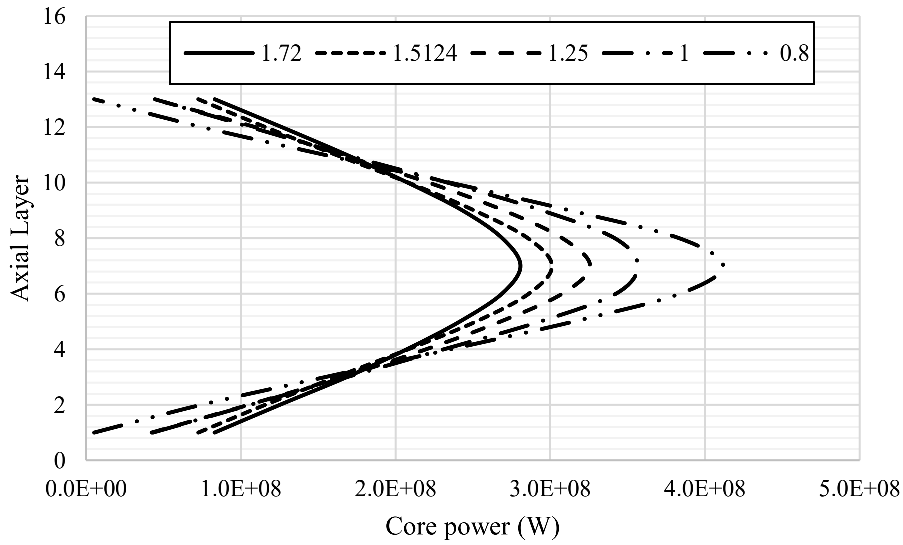

Fig. (11): Axial core power distribution at iteration 5 for different H/D

The 5th iteration, the power and temperature profiles for the developed models of the fuel rod ratios (1.72, 1.5, 1.25, 1.0, and 0.8) are compared. These five ratios share the same material composition specifications, but differ in fuel rod lengths within the core. The MCNP6/FLUENT calculations are conducted with 13 axial layers for each case. The final axial power profiles for all five ratios are shown in Figure 11.

The results showed that the power peak increases with decreasing H/D, where H/D is 1.72, 1.5, 1.25, 1 and 0.8 in the core.

The power peaking factor will calculate for each case. The result showed that the power peaking factor increases from 1.475 in the reference core (for the original length) case 1 to 1.64 in case 3 within the safety limits range. As seen from figure 12, the axial power peaking factor increases with decrease in H/D, where the highest core power peaking factor is for the smallest length (case 4 and case 5, where the fuel rod length is 249.08 and 200 cm) with the 1.7-1.95 range; they are out of safety limits 1.68-1.64. Thus, the fuel rod length is very effective in reducing the power peaking factor. From the five cases studied, the behavior of the peaking factor is acceptable for the only three cases with H/D ratios (1.72, 1.5, and 1.25).[14]

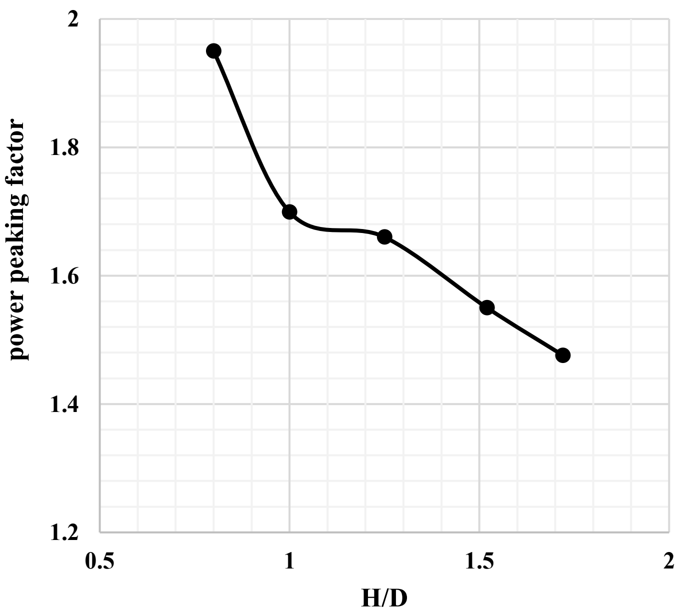

Fig. (12): Axial power peaking factor at iteration 5 for different H/D

Fuel, cladding, and coolant temperatures are estimated (as shown in figures 13, 14, and 15, respectively).

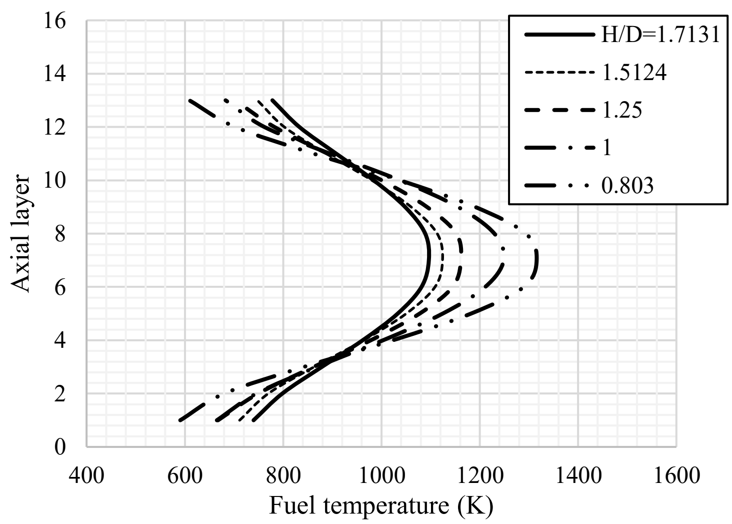

Fig. (13): Axial distribution of fuel temperature at iteration 5 for different H/D

Figure 13 shows the maximum fuel temperatures within the normal values at higher ratios (1.72, 1.5, and 1.25), where the maximum value at ratio 1.25 is 1161.4 K. On the other hand, at smaller ratios, the fuel temperature is higher, increase, reaching 1248.574 and 1315.6 K at H/D = 1.0 and 0.8, respectively, due to higher power (fig. 9) and hence higher cladding and coolant temperatures (fig.14 and 15).

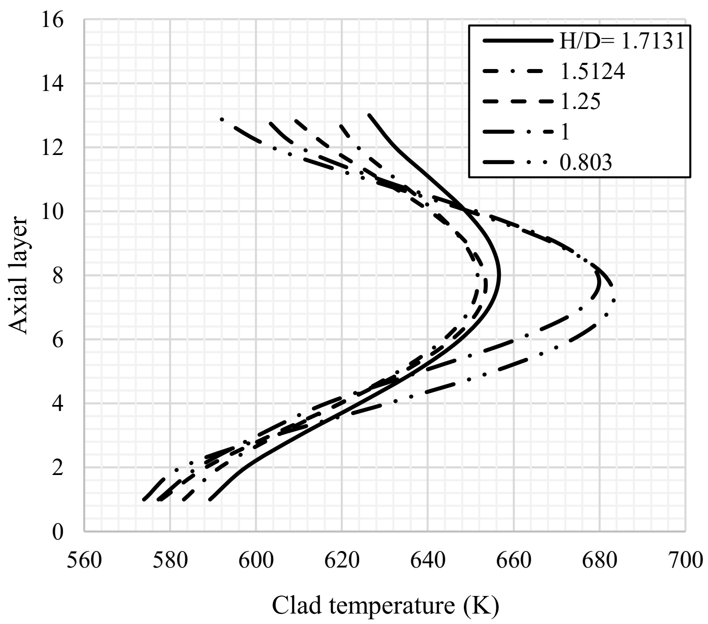

Fig. (14): Axial distribution of clad temperature at iteration 5 for different H/D

The cladding temperature at the first axial layer is 589 and the outlet layer 626 K, where the maximum value 657K at ratio 1.72 as shown in figure 14. Also, the maximum clad temperatures exceed 680 K in lower ratios.

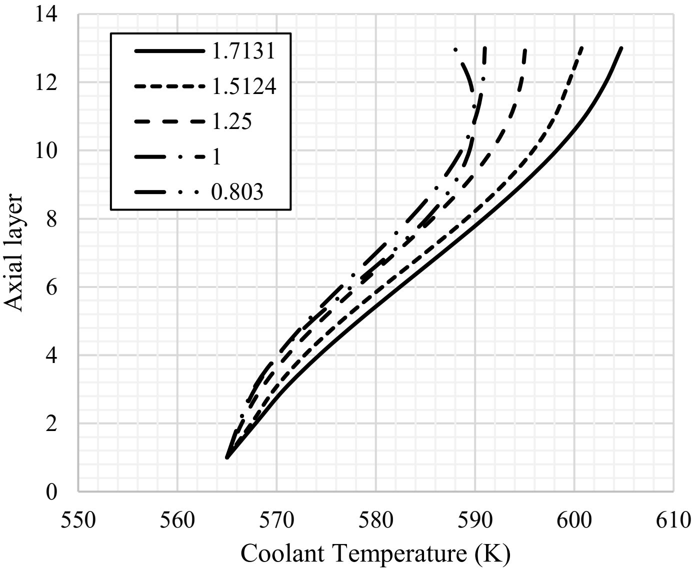

Fig. (15): Axial distribution of coolant temperature at iteration 5 for different H/D

Figure 15 shows the coolant inlet temperatures are the same for all H/D ratios (565K), where the outlet coolant temperature is lower at H/D = 1.0 and 0.8; the values are 590 and 587, respectively. The outlet coolant temperatures at higher ratios (1.72, 1.5, and 1.25) are 604, 600, and 595 K. to investigate the thermal power of the core; the core coolant temperature difference is plotted with H/D ratio.

Figure 16 shows the variation of the core coolant temperature difference (DT) with the H/D ratio. DT decreases with decreasing H/D as shown in figure where, the DT are 38.5, 34.5,30.7 ,25.9 and 21.0 oC with H/D 1.72,1.5, 1.25,1.0 and 0.8 respectively.

5.3-Mechanical Model

The mechanical model was integrated into a thermo-fluid and structural coupling framework. To streamline the process and reduce user effort, an extension tool was introduced to facilitate the transient load transfer from ANSYS Fluent to ANSYS Static Structural.

5.3.1 - Stress Analysis

The stress distribution was calculated based on the temperature results from the ANSYS Mechanical model. A geometric model of the fuel rod domain, created using simulation, was used as input for the ANSYS Static Structure module. All transfer results from the thermal module were applied as thermal loads on the cladding wall surface. The ANSYS Structural module then generates stress, strain, and damage results, which are analyzed for further study.

Table (3): The temperature difference and max. Stress with M% for variables H/D

H/D	DT-M%	Power Mw	DT-M%	Power Mw	*σ max %
1.7	**38.5-100%**	**1000***	-	-	original
1.5	**34.5-100%**	**897***	-	-	**-1%**
1.25	**30.7-100%**	**792***	-	-	**-2%**
1.0	25.5-100%	640	**32.2-80%**	**700***	**11%**
0.8	21-100%	517.5	**30.2-70%**	**550***	**12%**

*Affective at DT>30; M mass flow rate
DT temperature difference between inter and outlet of core

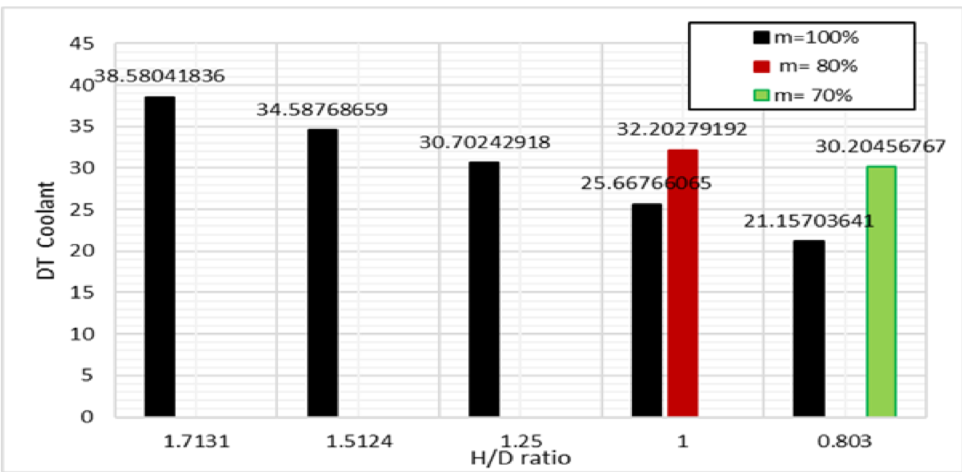

Fig. (16): the variation of coolant temperature difference with different H/D

Figure (17) shows the stress distribution along the fuel rod at M (mass flow rate) =100%, for the five lengths under studying, for the first three lengths (H/D= 1.7, 1.5, 1.25), the stress distribution is closed and the maximum stress reached to nearly 256-258 Mpa at the middle of the fuel rod, for the two lengths (H/D= 1, 0.8) the maximum stress is higher to 276Mpa., but for the two lengths (H/D= 1, 0.8), DT is less than 30 ^{0}C, which is not optimized for steam generator, so the M is modified to 80% for H/D=1, and modified to 70% for H/D= 0.8.

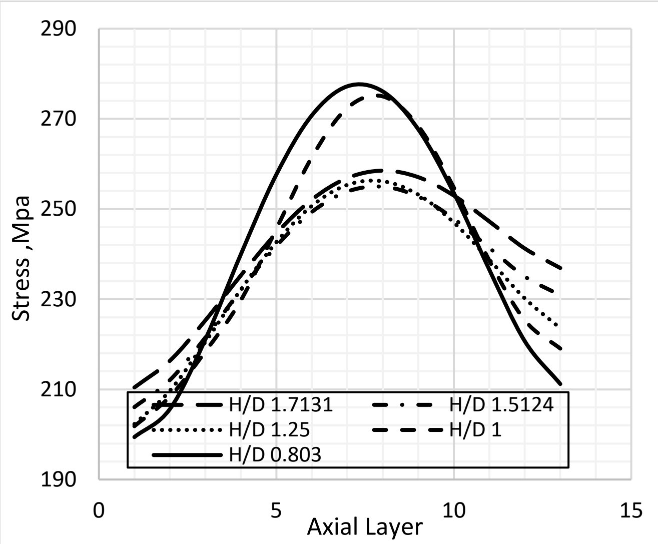

Fig. (17): the variation of axial cladding stress for different H/D at M=100%

In figures (18, 19), the maximum stress distribution for the modified M=80% at H/D=1 increases 4.91%, and for modified M=70% at H/D=0.8 increases 3.985%, that is due to the increase of the power.

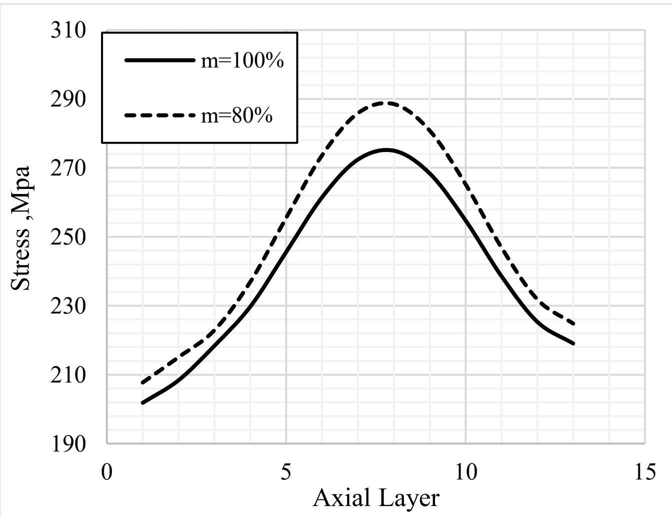

Fig. (18): the variation of axial cladding stress for H/D=1.0 at different M

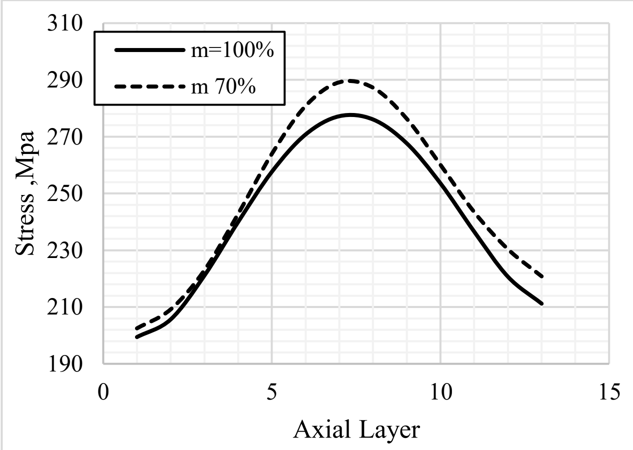

Fig. (19): the variation of axial cladding stress for H/D=0.8 at different M

Figure 20 shows the stress distribution for the five lengths with different mass flow rate, for H/D= 1.72, 1.5, 1.25, M=100%, for H/D= 1, M=80%, and for H/D=0.8, M= 70%.

These changed of mass flow rate occurred according to the length of fuel rod to achieve the DT=30^{0}C for the coolant, to reach the required power. After these changes, the Maximum stress for H/D= 1, 0.8 are highest to 287, 289 Mpa respectively, these changes are due to the change of mass flow rate, and the length of fuel rod.

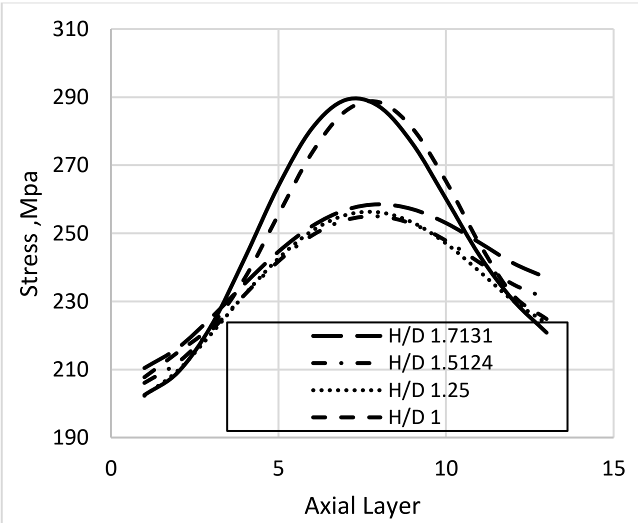

Fig. (20): the variation of axial cladding stress for different H/D at different M

The results showed from figures above, the first three lengths of fuel 1.7, 1.5, 1.25 are the best with respect to the temperature, power, stress distribution, and maximum stress. For the lengths 1, 0.8 the higher of stress leads to problems in clad of fuel rod.

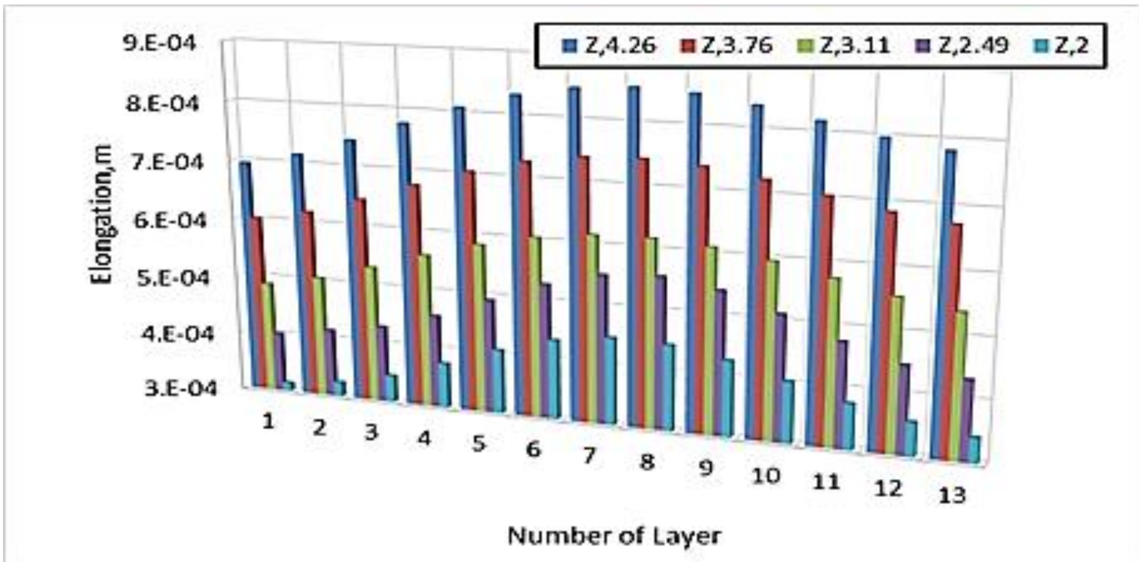

Fig. (21): Comparison between different H/D for the fuel rod elongation

Figure 21 shows the amount of elongation for each layer in the fuel rod, the maximum elongation occurred at layers (7, 8, and 9), reached to 8.55E-4 m, for maximum length, and reached to 4.45E-4 m, for minimum length. The elongation increases due to the increasing of temperature of fuel rod, the longest fuel rod gives the higher power, due to the mass fuel, so it gives the higher elongation.

CONCLUSIONS

Neutronic and thermal hydraulic models using (MCNP6–ANSYS Fluent), followed by the ANSYS-STATIC structure module, are created to simulate IRIS five cases with different fuel rod lengths (426.72, 376.7, 311.5, 249.08, and 200 cm), with ratios (H/D = 1.72, 1.5, 1.25, 1.0, and 0.8), respectively. The calculations are repeated until the required convergence criteria of safety parameters are fulfilled at iteration 5.

Then calculations are performed to study the effect of different fuel rod lengths on the safety parameters of the IRIS reactor core. The results showed that the axial power increases with decreasing H/D, and from the five cases studied, the behavior of the power peaking factor is acceptable for only three cases with H/D ratios (1.72, 1.5, and 1.25).

The longest length gives the highest heat exchange that longer fuel rods have greater surface area, improving heat transfer thus giving the best stress distribution along the fuel rod, because longer rods allow more gradual temperature distributions, leading to more uniform thermal stress, despite the increased energy generated. So, the temperature difference across each core is decreasing with decreasing the length of the fuel rod; thus, the core power is decreasing.

The results concluded that the length of the fuel rod must not be less than 311.5 cm, and therefore the ratio must not be less than 1.25 to avoid the increasing of stresses at the middle of the fuel rod, which may lead to deformation occurring in part of the fuel rod.

REFERENCES

[1] Canhui SUN, Ning BAI, Di ZHANG and Yaodong CHEN "Analysis of Thermal-Hydraulic Behavior for Reduced-Height PWR Fuel Assemblies" State Power Investment Corporation Research Institute, Beijing 102209, China, ICONE 2017.

[2] Varin, E, Marleau, G, and Chambon, R. Transport-diffusion coupling for Candu reactor core follow-Up., International conference on supercomputing in nuclear applications SNA'2003, Paris (France), 22-24 Sep 2003.

[3] J. Hu and R. Uddin, "Coupled Neutronics and Thermal-Hydraulics Using MCNP and FLUENT," Transactions of the American Nuclear Society, Vol. 98, pp. 606-608 (2008).

[4] Refeat, Riham M., Refaey, Ahmed M. and Abdel-Latif, Salwa H. "Coupling MCNP6/ANSYS codes to calculate axial temperature and power distribution in a VVER-1000 fuel assembly" Kerntechnik, vol. 87, no. 3, 2022, pp. 323-335. https://doi.org/10.1515/kern-2021-1065

[5] N. Cardoni, "Nuclear reactor multi-physics simulations with coupled MCNP5 and STAR-CCM+". Diss. University of Illinois (2011).

[6] Neil E. Todreas and Mujid S. Kazimi (1990), NUCLEAR SYSTEMS I Thermal Hydraulic Fundamentals, Massachusetts Institute of Technology, USA ,Taylor & Francis, second printing. 1990, 512 pages, ISBN 1-56032-936-9 (case), ISBN 1-56032-079-6.

[7] D. Weber, T. Sofu, D. Pointer, A. Tentner, Z. Zhong, T. Downar, J. Thomas, S. Lo, A. Splawski, "Extension of Integrated Neutronic and Thermal-Hydraulic Analysis Capabilities of the Numerical Nuclear Reactor Software System for BWR Applications," Proceedings of PHYSOR-2006, Vancouver, BC, Canada, September 10-14 (2006).

[8] M.D. Carelli et al. "The design and safety features of the IRIS reactor", Nuclear Engineering and Design 230, 151–167. (2004)

[9] Petrovic,B., IRISNeutronics/Core Design Benchmark Problem Specification – Benchmark 44: Core Depletion Analysis without Feedback," Report IRIS-WEC- 12 (Rev.2) pp.33, Westinghouse,2002.

[10] Pelowitz. B. MCNP6 User's Manual Version 1.0. Los Alamos National Laboratory report, LA-CP-13-00634, Rev. 0, (2013).

[11] August ANSYS, 2016. ANSYS Fluent User's Guide, 17.2, Release (2016).

[12] Chadwick, M. B., Herman, M. W., Oblozinsky, P., Dunn, M. E., Danon, Y., Kahler, A., Smith, D., Pritychenko, B., Arbanas, G., Arcilla, R., Brewer, R., Brown, D. A., Capote, R., Carlson, A. D., Cho, Y. S., Derrien, H., Guber, K. H., Hale, G. M., Hoblit, S., and Shannon, T. "ENDF/B-VII.1 Nuclear Data for Science and Technology: Cross Sections, Covariance, Fission Product Yields and Decay Data." Nuclear Data Sheets 112 (12): 2887-996, 2011.

[13] Bahdanovich, R.B., Bogdanova, E.V., Gamtsemlidze, I.D.,Nikonov, S.P., and Tikhomirov, G.V. Test case for VVER-1000 complex modeling using MCU and ATHLET. IOP Conf. Ser. J. Phys. Conf. 781: 012050, (2017).

[14] IAEA-TECDOC-1536, Status of Small Reactor Designs without on-Site Refuelling: 2007.